Overheating prevention in solar collectors using a hybrid predictive controller

Adriano Silva Martins Brandão[1], Paulo Renato da Costa Mendes[1], Tiago de Araújo Elias[1] and Julio Elias Normey-Rico[1]

[1] Federal University of Santa Catarina, Florianópolis (Brazil)

Abstract

This paper proposes a new method for avoiding overheating of the heat transfer fluid on solar thermal energy collectors. The proposed strategy is based on a combination of partial and total defocusing of the collectors in a single Practical Nonlinear Model Predictive Control structure. Simulation results are used to show the advantages of the proposed formulation The controller is evaluated with an high accurate simulation setup and it is shown that the hybrid controller incorporates the reference tracking performance and decreased computation times of the combined controller formulations and capable of maintaining high energy absorption on scenarios of pump failures and undetected changes on mirror efficiency.

Keywords: Overheating control, solar energy, Practical nonlinear model predictive control, Solar collector defocusing

1. Introduction

The importance of solar energy to solve the energetic sustainability issues of the current era is very significant due to the abundance of this energy source, therefore the development of solar energy collection and transformation is encouraged (Andrade et. al. 2013). There are some important operational constraints to be considered with solar thermal applications, especially the maximal allowable temperature on the Heat Transfer Fluid (HTF). These temperature limits are defined by the fluid properties and by constructive characteristics of the plant. If these temperatures are reached, the HTF can decompose, generating inflammable gases and causing premature component failures, reducing the system performance (Frank, 2015) and compromising its safety. As such, avoiding the operational upper bounds for temperatures constitutes an interesting control problem, as the solar collector should provide the biggest energy output possible while maintaining the integrity of the processes' components.

This work focuses on the control of a solar collector field, which is composed of several parallel collector loops. A solar collector loop is composed of several solar energy collectors connected in serial configuration. Each collector is composed of a reflector that focuses the sun irradiation on an absorber tube. Inside the absorber tube, a Heat Transfer Fluid flows through the collector loop and recieves the thermal energy from the absorber tube. The amount of energy that the HTF has at the output of the loop is directly related to the amount of solar irradiation at the reflectors, which is both the main source of energy for the process and its main disturbance, and the degree of focus of the reflector. Typical control structures only manipulate the HTF flow as it changes the amount of energy absorbed per unit of time, but the defocusing of the reflector mirrors introduces a degree of freedom to the control structure and allows for faster lowering of the HTF temperature.

The control strategy applied to this process must be capable of maintaining the process under operational constraints, such as the maximum temperature allowed for the HTF, while maintaining the power generation (Sánchez et. al. 2018). This type of process has very few degrees of freedom for the control actions as the HTF flow is typically the only manipulated variable and the collectors are only defocused for safety concerns. In a previous work, Elias et. al. (2019) proposed two defocusing strategies in order to keep the HTF temperature under the operational constraints while maintaining the desired energy output: on/off and partial defocusing of the collectors. This work aims integrating both defocusing strategies in a centralized Nonlinear Model Predictive

doi:10.18086/swc.2019.18.02 Available at http://proceedings.ises.org

Control (NMPC) framework in order to obtain the best aspects from both previous controllers.

2. Process Model

The model utilized in this work is a lumped parameter model for each collector of the solar field, shown by Elias et. al. (2019), and is based on the distributed parameter model proposed by Carmona (1985). The expression for the output temperature of HTF at each collector is given by eq. 1:

$$\rho_f c_f A_f \dot{\mathrm{T}}_{\mathrm{out}_{\mathrm{i,j}}}(\mathrm{t}) = \frac{\varphi_{out_{i,j}}(t)}{10} \eta_o G \Phi\!\downarrow(t) - \rho_f c_f \frac{v_i(t-d_c)}{n_C} \frac{\mathrm{T}_{\mathrm{out}_{\mathrm{i,j}}}(\mathrm{t}) - \mathrm{T}_{\mathrm{in}_{\mathrm{i,j}}}(\mathrm{t})}{\mathrm{L}} - \frac{H_l\left(\mathrm{T}_{\mathrm{out}_{\mathrm{i,j}}}, \mathrm{T}_{in_{\mathrm{i,j}}}, T_a\right)}{Lt} \quad \text{(eq. 1)}$$

where $\mathrm{T}_{\mathrm{out}_{\mathrm{i,j}}}$ and $\mathrm{T}_{\mathrm{in}_{\mathrm{i,j}}}$ are respectively the output and input temperatures of the HTF at collector j of loop i, v_i is the volumetric flow of the HTF considering equal flow in every collector of the loop i, H_l is a function for the thermal losses of the collector and G is the optical aperture of the mirror and $\varphi_{out_{i,j}}$ the current focus state of the collector j at loop i, with values ranging from 0 to 10. The value 0 represents a completely defocused collector, the value 3 represents a collector with 30% focus while the value 10 represents a completely focused collector. A description of the parameters of the model are presented on Tab. 1.

Tab. 1: Parameters of the model.

Symbol	Description	Unit
A_f	Absorber section	m^2
c_f	Specific heat of fluid	$J\ kg^{-1}\ K^{-1}$
H_l	Function of thermal losses	$J\ s^{-1}\ K^{-1}$
L	Solar collector length	m
Lt	Loop length	m
η_o	Mirror optical efficiency	
G	Mirror optical aperture	m
ρ_f	Density	$kg\ m^{-3}$

Specific heat and specific mass of the HTF are dependent on the temperature and for the considered thermal fluid are given by eq. 2 and eq. 3:

$$\rho_f(\mathrm{t}) = 903 - 0.672 \frac{\mathrm{T}_{\mathrm{out}_{\mathrm{i,j}}}(\mathrm{t}) + \mathrm{T}_{in_{\mathrm{i,j}}}(t)}{2} \quad \text{(eq. 2)}$$

$$c_f(\mathrm{t}) = 1820 - 3.76 \frac{\mathrm{T}_{\mathrm{out}_{\mathrm{i,j}}}(\mathrm{t}) + \mathrm{T}_{in_{\mathrm{i,j}}}(t)}{2} \quad \text{(eq. 3)}$$

As the defocusing of the collectors involves the movement of mechanical parts such as mirrors, there is a dynamic to be considered for changes on the focus. This actuation dynamic is modeled as a first order differential equation with unitary static gain and a time constant τ_{A} as shown on eq. 4:

$$\tau_A \dot{\varphi}_{out_{i,j}}(t) = -\varphi_{out_{i,j}}(t) + \varphi_{i,j}(t) \quad \text{(eq. 4)}$$

where $\varphi_{i,j}$ is the focus value calculated by the controller and applied by the actuator j of loop i.

As the collectors are connected in serial configuration on each loop, the output temperature of the previous collector is the input collector of the next and the output temperature at the last collector of a loop is the output temperature of the loop. The loops are connected in parallel configuration and as such the output temperature of the whole field ($T_{out_{field}}$) is calculated as a weighted average of the output temperatures for each loop and the volumetric flow. It is also considered a first order dynamic for the mixing of the flows from each loop, similarly to the focus actuators. Considering a collector field composed of n_L parallel collector loops with n_c collectors each, eq. 5 expresses a model for the output temperature for the whole field.:

$$\tau_{\mathrm{T}} \dot{T}_{\mathrm{out}_{\mathrm{field}}}(t) = -T_{out_{field}}(t) + \frac{\sum_{i=1}^{n_L} T_{out_{i,ns}}(t) v_i(t)}{\sum_{i=1}^{n_L} v_i(t)} \quad \text{(eq. 5)}$$

where τ_{T} is the time constant considered for the mixing of the flows.

As pointed out by Elias et. al. (2019), this model has good performance for control purposes and therefore is used in this work as the prediction model of the controller and the process to be controlled.

3. Model Predictive Control Principles

The term Model Predictive Control (MPC) refers not only to a specific control strategy, but to a family of algorithms based on prediction and optimization. With MPC, at each sampling time the foreseeable future behavior of the controlled variables is predicted in a prediction horizon, provided a process model, measurements and future control actions (Camacho and Bordons, 2007). These future control actions are proposed by an optimizer, which tries to obtain the control movements that best reaches the provided objective while respecting the imposed constraints. One of the main reasons for the success of MPC applications is its native capacity to handle multivariable coupled dynamics with constrains, allowing the control of complex processes such as a solar collector field. A diagram showing the main elements of MPC are presented on fig. 1.

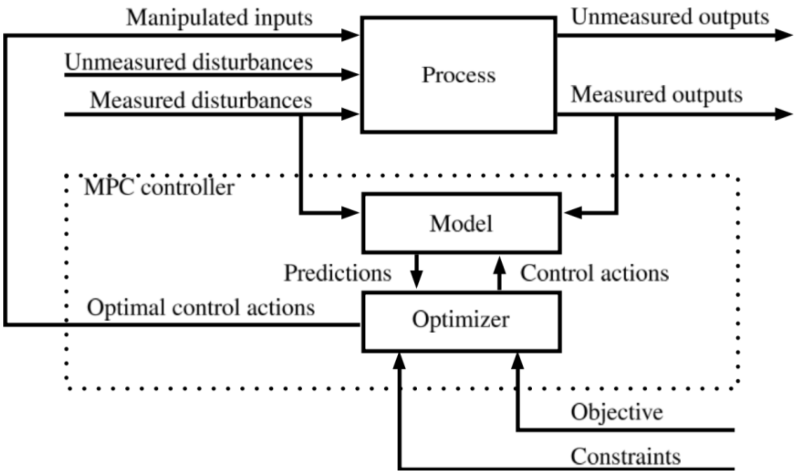

Fig. 1: Basic structure and elements of MPC.

One of the main limitations on the implementation of MPC controllers is the computation time of the optimization problem to be solved, which must be completed in a single sampling time. at each iteration. As such, it is usual to formulate convex problems, that can be solved fast and reliably due to the existence of robust numerical methods for solving these problems. The inclusion of integer and binary variables can increase the computation complexity and therefore must be studied in order to evaluate the feasibility of implementation.

Another aspect that can affect the computation times of the controller is the prediction of the controlled variables. The complexity of the model used for predictions can greatly increase the computation times of the controller as nonlinear models can take much time to be evaluated and make the optimization problem not convex. To solve this issue, linear models are frequently used as they require little computation to be evaluated and facilitate the formulation of a convex problem. The predictions ($\boldsymbol{Y}$) from these linear models can be rewritten as a sum of two terms: free response and forced response, as seen on eq. 6.

$$\boldsymbol{Y} = G.\Delta\boldsymbol{U} + \boldsymbol{f} \quad \text{(eq. 6)}$$

The free response, represented by $\boldsymbol{f}$**,** is the predicted output of the model given that no change is applied to the manipulated variables on the prediction horizon. The forced response, given by the term $G.\Delta\boldsymbol{U}$, represents the predicted output of the model given a stationary state at the beginning of the prediction horizon and the future control actions proposed by the controller ($\Delta\boldsymbol{U}$). The matrix G, called dynamic matrix, is obtained from the linear model parameters.

The use of linear models can limit the operational region of the controller due to the increasing modeling errors when the process goes to regions distant from the linearization point of the model. In order to increase the region in which the prediction model is valid, Nonlinear MPC techniques use nonlinear models to predict the process. In order to avoid the issues associated with the use of nonlinear models, there are algorithms such as the Practical Nonlinear Model Predictive Control (PNMPC) proposed by Plucênio et. al. (2007) that obtain a new linear model from the nonlinear model at each iteration of the controller, allowing for fast calculations and formulation of convex optimization problem. The PNMPC also uses the nonlinear model to compute the free response, allowing for a better representation of the process dynamics on the predictions.

4. Control Structure

The proposed hybrid control structure aims to manipulate the HTF flow within its operational range to achieve the reference tracking objective. The controller should also defocus the solar collectors when the maximum HTF temperature is to be reached in a predictable future horizon while considering the future reference trajectory for the HTF temperature and the disturbances of ambient temperature, irradiation, and inlet temperature. These control objectives are accomplished using PNMPC.

2.1. Proposed control formulation

The specification of the MPC controller involves the definition of an optimization problem, which consists of an objective function and constraints. The objective-function to be minimized by the proposed controller is divided in three terms, as expressed in eq. 7:

$$J = J_1 + J_2 + J_3 \qquad \text{(eq. 7)}$$

The terms J_1, J_2 and J_3 represent three conflicting objectives of the controller: Tracking of a reference for the solar field output temperature, given by eq. 8; Minimization of the movement of the manipulated variables, given by eq. 9; and Maximization of the volumetric flow of HTF and focus value in order to indirectly maximize the energy output of the process, given by eq. 10.

$$J_1 = \sum_{N}^{k=1} \left(T_{out_{field}}(t+k) - T_{ref}(t+k) \right)^2 \boldsymbol{Q_T} \qquad \text{(eq. 8)}$$

$$J_2 = \sum_{N_c}^{k=1} \sum_{n_L}^{i=1} (\Delta v_i(t+k))^2 \boldsymbol{R_v} + \sum_{N_c}^{k=1} \sum_{n_c}^{j=1} \sum_{n_L}^{i=1} \left(\Delta\varphi_{i,j}(t+k) \right)^2 \boldsymbol{R_\varphi} \qquad \text{(eq. 9)}$$

$$J_3 = -\sum_{N_c}^{k=1} \sum_{n_L}^{i=1} \left(v_i(t+k) \right)^2 \boldsymbol{Q_v} - \sum_{N_c}^{k=1} \sum_{n_c}^{j=1} \sum_{n_L}^{i=1} \left(\varphi_{i,j}(t+k) \right)^2 \boldsymbol{Q_\varphi} \qquad \text{(eq. 10)}$$

Where $\mathrm{T}_{\mathrm{out}_{\mathrm{field}}}$ and T_{ref} are the predicted and reference outlet temperatures of the solar field for the prediction horizon, Δv_i the changes on the flow of each loop of the solar field for the control horizon of this variable, $\varphi_{i,j}$ the focus variable for all collectors of each loop of the field for the control horizon of this variable and $\Delta\varphi_{i,j}$ the changes on $\varphi_{i,j}$ for the same control horizon. The square matrices $\boldsymbol{Q_T}$, $\boldsymbol{Q_v}$, $\boldsymbol{Q_\varphi}$, $\boldsymbol{R_\varphi}$ and $\boldsymbol{R_v}$ are weights of appropriate size. The prediction horizon is given by N while the control horizon is given by N_c

The two control strategies that are combined on this work will be referred to as On/Off, where the controller should completely defocus a collector if the outlet temperature of any collector gets above the upper limit over the prediction horizon of the controller; and Partial, where the controller combines the manipulation of flow and partial defocusing of the collector in order to achieve the control objectives with smaller control effort when compared to the On/Off case.

In order to implement the proposed integrated strategy, it is necessary to introduce the binary variable δ_i which indicates if a collector i should be focused ($\delta_i = 1$) or completely defocused ($\delta_i = 0$). The constraints presented in eq. 11 and 12 determine the possible values of the focus $\varphi_{i,j}$ and its change rate $\Delta\varphi_{i,j}$.

$$0 \le \varphi_{i,j}(\mathrm{t}+\mathrm{k}) \le 10\delta_{i,j} \qquad i = 1..n_L, j = 1..n_c, k = 1..N_c \qquad \text{(eq. 11)}$$

$$-\delta_{i,j}(t+k) - 10\left(1 - \delta_{i,j}(t+k)\right) < \Delta\varphi_{i,j}(t+k) < \delta_{i,j}(t+k) + 10\left(1 - \delta_{i,j}(t+k)\right)$$
$$i = 1..n_L, j = 1..n_c, k = 1..N_c \qquad \text{(eq. 12)}$$

If the collector is to be focused ($\delta_{i,j} = 1$), the focus value has full range between 0% focus ($\varphi_{i,j} = 0$) to 100% focus ($\varphi_{i,j} = 10$) and the change in focus is limited to ±10% ($-1 < \Delta\varphi_{i,j} < 1$) but if the collector should be completely defocused ($\delta_{i,j} = 0$), the focus value is forced to be zero and the change in focus can range from -100% to 100% as it should be capable going form completely focused to defocused and vice versa.

As stated by Elias et. al. (2019), there are operational limits for the HTF flow (v_{MAX} and v_{MIN}) and in order to prevent the controller from manipulating the flow rate when the collector is defocused, the constraints presented in eq. 13 are applied, which forces the applied flow to be at the upper limit when the collector is defocused ($\delta_{i,j} = 0$).

$$\begin{cases} v_i(t+k) \leq v_{MAX} \\ v_i(t+k) \geq v_{MIN}\delta_{i,j}(t+k) + v_{MAX}\left(1-\delta_{i,j}\right) \end{cases} \quad i = 1..n_L, j = 1..n_c, k = 1..N_c \qquad \text{(eq. 13)}$$

In order to determine if a collector should be defocused, the binary variable $\alpha_{i,j}$ is introduced to indicate if, in a given time of the prediction horizon, the HTF temperature at collector j exceeds the maximum allowed temperature ($\alpha_{i,j} = 0$) or not ($\alpha_{i,j} = 1$). This condition is expressed in eq. 14:

$$\alpha_{i,j}(t+k-1|t) = 1 \leftrightarrow \hat{T}_{out_{i,j}}(t+k|t) \leq T_{max} \qquad i = 1..n_L, j = 1..n_c, k = 1..N \qquad \text{(eq. 14)}$$

Where $\hat{T}_{out_{i,j}}$ is the prediction for the outlet temperature of collector j from loop i. This condition can be rewritten as the inequalities presented in eq. 15 when considering that the flow is at the upper limit when the collector is defocused.

$$\begin{cases} \alpha_i(t+k-1|t)\hat{T}_{out_{i,j}}|_{v=v_{MAX}}(t+k|t) - T_{max} \leq 0 \\ \hat{T}_{out_{i,j}}|_{v=v_{MAX}}(t+k|t) - \left(1-\alpha_{i,j}(t+k-1|t)\right)T_{max} \geq 0 \end{cases} \quad i = 1..n_L, j = 1..n_c, k = 1..N \qquad \text{(eq. 15)}$$

The decision to completely defocus a collector ($\delta_{i,j} = 0$) is to be taken if in any instant of the prediction horizon, the predicted outlet temperature of the collector is above the upper limit for the HTF, as expressed in the inequalities of eq. 16:

$$\begin{cases} -\alpha_{i,j}(t|t) + \delta_{i,j}(t|t) \leq 0 \\ -\alpha_{i,j}(t+1|t) + \delta_{i,j}(t|t) \leq 0 \\ \vdots \\ -\alpha_{i,j}(t+N_\alpha-1|t) + \delta_{i,j}(t|t) \leq 0 \\ \alpha_{i,j}(t|t) + \alpha_{i,j}(t+1|t) + \cdots + \alpha_{i,j}(t+N_\alpha-1|t) - \delta_{i,j}(t|t) - N_\alpha + 1 \leq 0 \end{cases}$$

$$i = 1..n_L, j = 1..n_c, k = 1..N \qquad \text{(eq. 16)}$$

5. Results and Discussion

In order to evaluate the performance of the hybrid controller and compare with the On/Off and Partial defocusing controllers, three simulation scenarios were created:

- High irradiation scenario: An irradiation profile for the morning of a day with high peak irradiation and some clouds;
- Pump failure scenario: An irradiation profile for the start of the afternoon with no clouds. At two moments on the simulation, a malfunction is simulated on the pump for loop 1 of the solar field and the flow is fixated. Between $t = 36\ min$ and $t = 54\ min$ the flow at loop 2 was locked at 8 $10^{-3}\ m^3s^{-1}$ and between $t = 132\ min$ and $t = 156\ min$ the flow at loop 2 was locked at 12 $10^{-3}\ m^3s^{-1}$.
- Mismatch pump failure scenario: The same as the previous case with the introduction, but an 10% error is introduced on the optical efficiency parameter.

The applied profiles for ambient temperature and irradiation are presented on fig. 2 and 3. In order to evaluate the simulated results, three performance indexes were considered: Amount of heat absorbed by the HTF, the integral of the squared reference tracking error (ISE) for the output temperature of the solar field, and the average computation time for the controllers. The results are presented on Tab. 2.

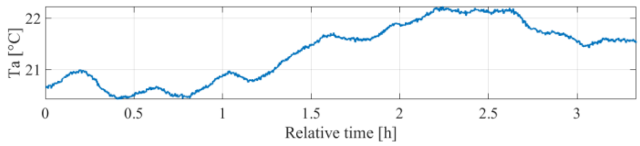

Fig. 2: Ambient temperature profile used on all cases.

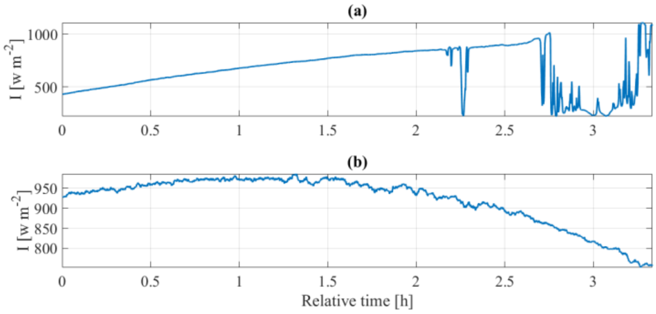

Fig. 3: Irradiation profiles: (a) High irradiation profile; (b) Pump failure profile.

Tab. 2: Performance indices for the simulated cases

		On/Off	**Partial**	**Hybrid**
1 - High irradiation scenario	Heat [J]	3.8723e+09	4.6064e+09	3.5178e+09
	ISE	5.8366e+04	4.4523e+04	9.2163e+04
	Mean time [s]	0.6728	0.0617	0.1367
2 - Nominal case with pump failure	Heat [J]	4.8853e+09	3.7994e+09	4.8700e+09
	ISE	3.5497e+04	4.3240e+04	3.7473e+04
	Mean time [s]	0.7406	0.1178	0.0967
3 - Mismatch case with pump failure	Heat [J]	5.3123e+09	3.9164e+09	5.3761e+09
	ISE	4.6513e+04	3.9734e+04	4.3900e+04
	Mean time [s]	0.6461	0.1128	0.1227

Results for the simulations of the high irradiation scenario are shown in figures 4, 5 and 6. These figures present the output temperature of the whole field and it's reference, the focus value for each collector and the HTF flow for both loops. As the partial defocusing controller kept the flows high when compared to the other controllers, the amount of thermal energy absorbed by the HTF is greater for this controller (see Tab. 2). The Hybrid controller presented small changes on the flow, which resulted on greater variability of the output HTF temperature and elevated values of ISE. In this case, the Hybrid controller presented itself as less aggressive when compared to the other MPC, which is desirable for reducing the wearing of actuators, but may result on losses on energy absorption efficiency. The partial and hybrid controllers presented smaller computation times when compared to the On/Off controller, as the optimization problem solved by this controller is more complex.

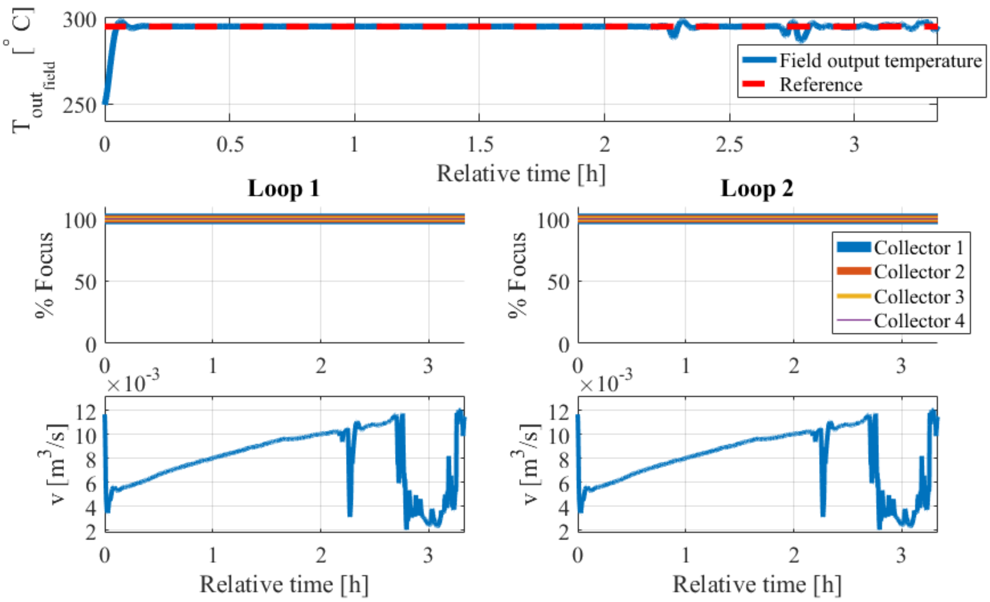

Fig. 4: Simulation results for the On/Off controller at the nominal case with high irradiation.

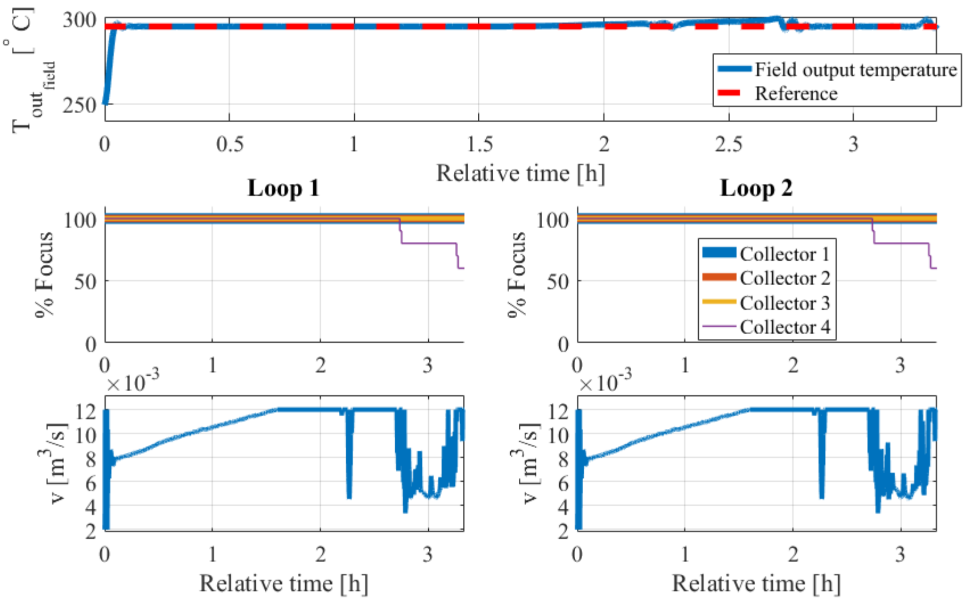

Fig. 5: Simulation results for the partial focus controller at the nominal case with high irradiation.

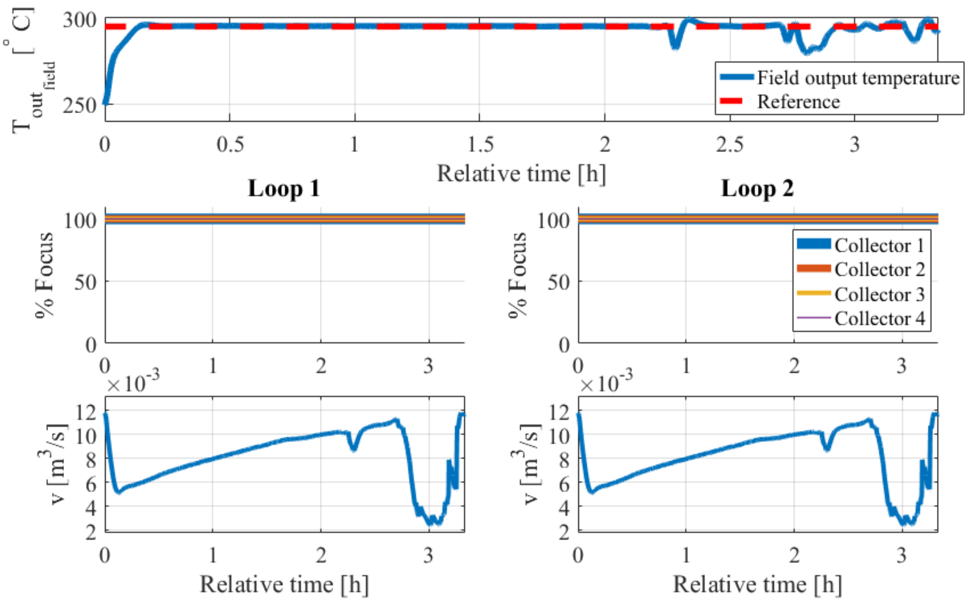

Fig. 6: Simulation results for the Hybrid controller at the nominal case with high irradiation.

The results for the pump failure scenario are presented on figures 7, 8 and 9. As shown in figure 9, it is possible to see that the hybrid controller generates smaller deviations from the reference temperature when compared to the other MPC, during the pump malfunctions. It is also notable that during both pump malfunctions, the hybrid controller managed to converge the proposed control action to the fixed flow values. This did not happen on the other controllers, with the On/Off (Fig. 7) proposing different flow values during the first pump failure and the partial controller (Fig. 8) proposing different flow values at the second pump failure. It is important to note that the switching observed on the On/Off controller (Fig. 7) is undesired and is result of failure to obtain a online feasible solution for the optimization problem. The partial controller defocused two collectors on both loops for almost all the simulation, as seen on figure 8. This is not desirable because if there is no overheating risk, defocusing the collector decreases the amount of energy that can be absorbed by the HTF, as can be seen when comparing the amounts of absorbed heat on Tab 2. For this simulation case, the computation times had similar behavior to the previous case, with the On/Off controller taking more time to compute the control actions.

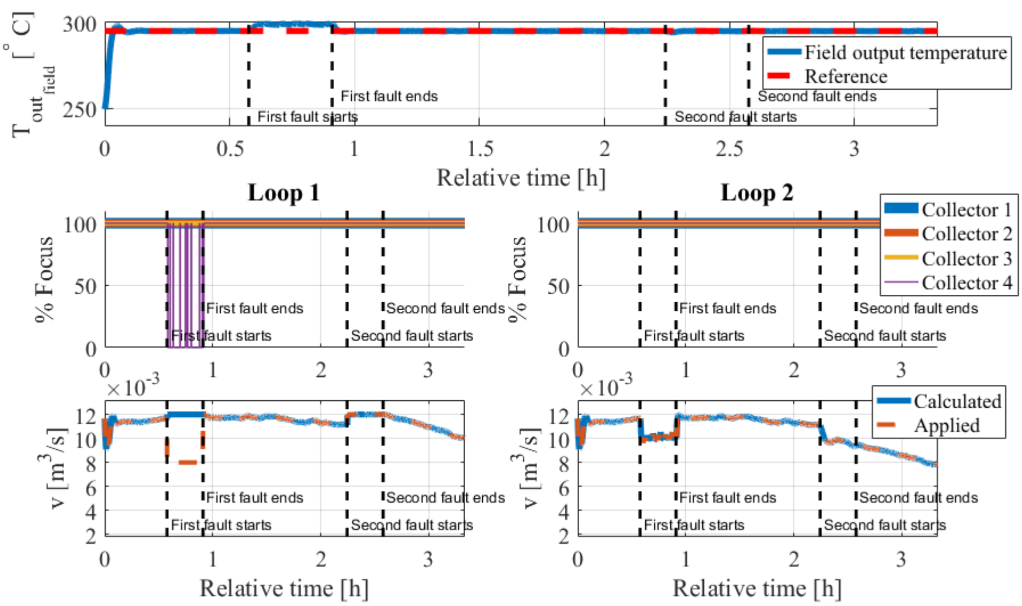

Fig. 7: Simulation results for the On/Off controller at the nominal case with pump failure.

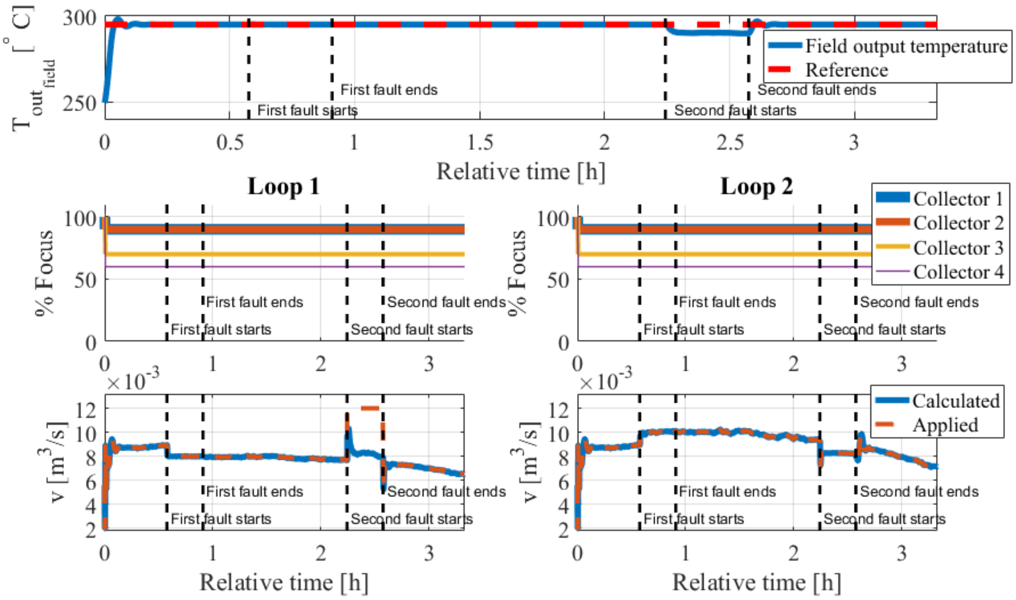

Fig. 8: Simulation results for the partial focus controller at the nominal case with pump failure.

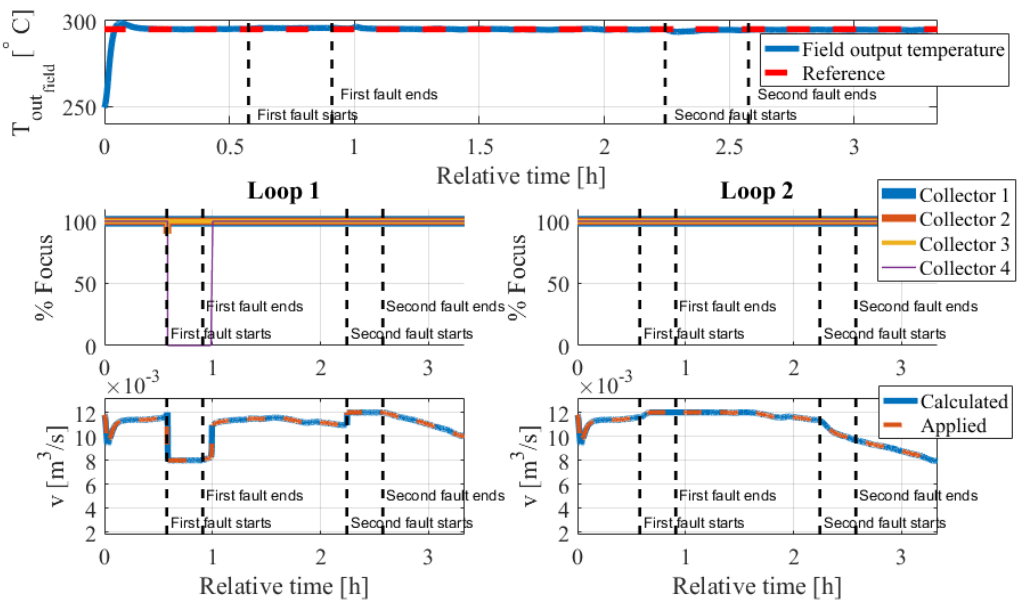

Fig. 9: Simulation results for the Hybrid controller at the nominal case with pump failure.

The results for the pump failure scenario with model mismatch are presented on figures 10, 11 and 12. In this simulation case, it is possible to see that the partial focus controller (Fig. 11) used lower flow values during the simulation, resulting on less energy being absorbed by the HTF (Tab. 2). The On/Off and Hybrid controllers presented similar amounts of energy absorbed, but with much smaller computation times and better reference tracking. The defocusing presented on the Hybrid controller (Fig. 12) is considerably grater than the one calculated by the On/Off controller (Fig. 10), as the latter has constraints to avoid excessive switching.

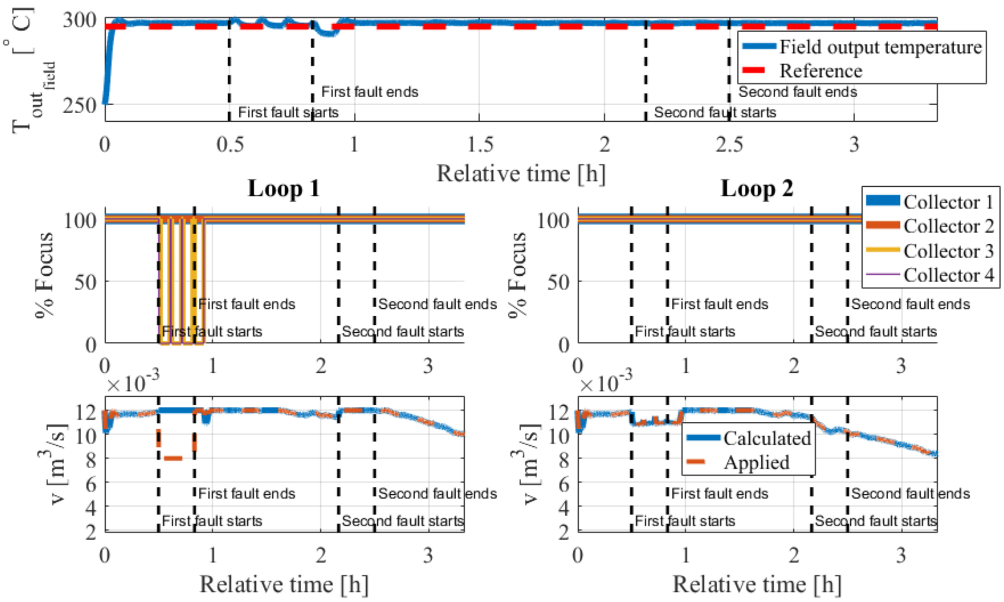

Fig. 10: Simulation results for the On/Off controller at the nominal case with pump failure.

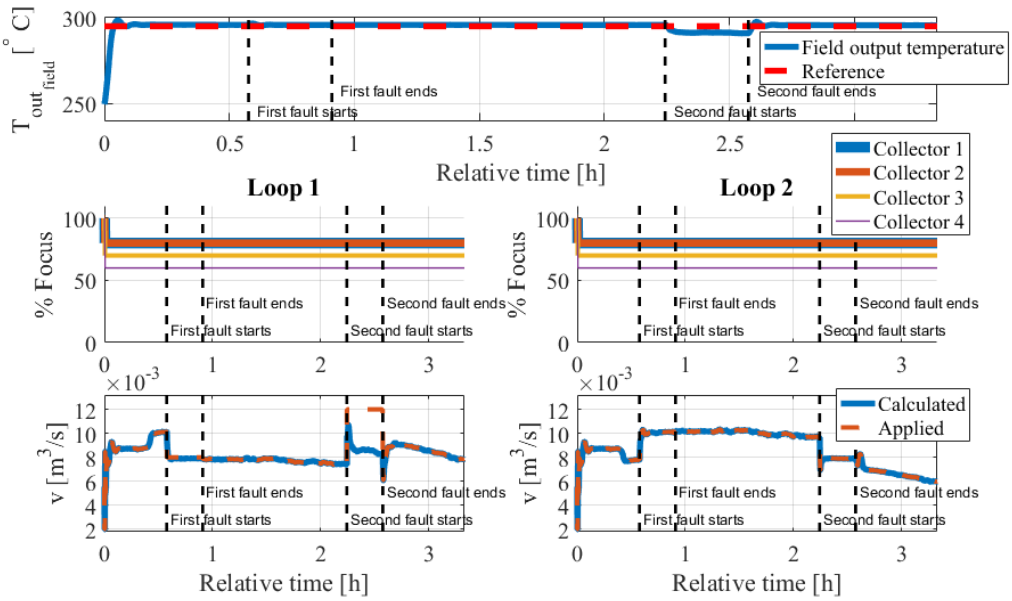

Fig. 11: Simulation results for the partial focus controller at the nominal case with pump failure.

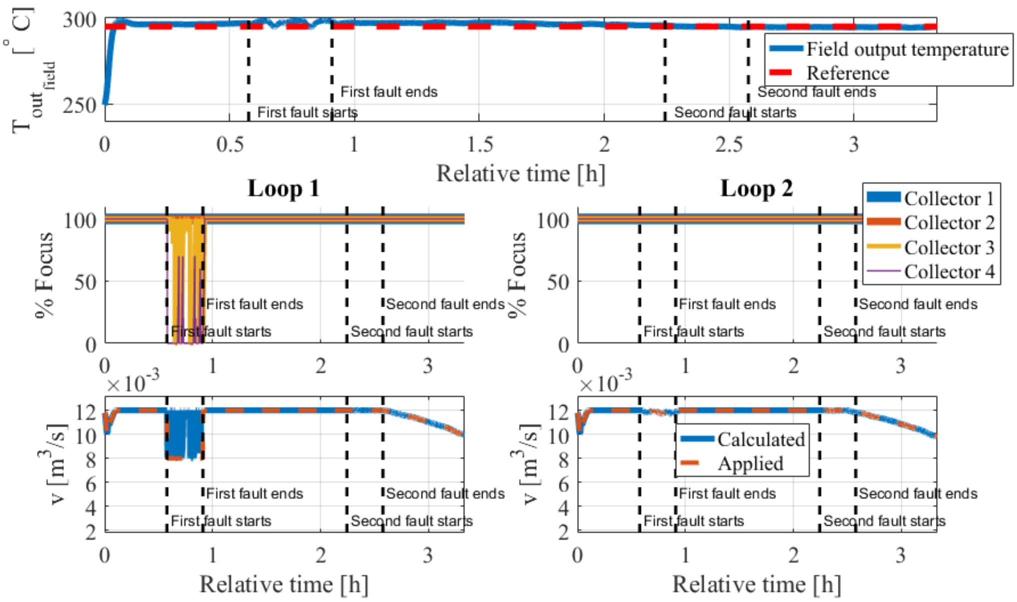

Fig. 12: Simulation results for the Hybrid controller at the nominal case with pump failure.

It is important to point out that the behavior of MPC controllers is highly dependent on the tuning parameters. The tuning of the controllers analyzed on this paper was complex, especially for the hybrid controller, as its objective function contained several conflicting objectives with various variables that have very different ranges of possible values.

6. Conclusions

This paper presented a hybrid MPC algorithm for overheating prevention on a solar collector field that manipulates flow and focus values. The controller combined two previous MPC formulations that apply partial and On/Off defocusing of the collectors and is based on the PNMPC controller. The resulting Mixed-Integer optimization problem is then solved at each iteration of the controller in order to obtain optimal control actions.

These controllers were compared through simulating a two-loop solar collector field with a high accuracy process model. Irradiation and ambient temperature profiles used in the simulation were obtained from experimental data. Three simulation scenarios were evaluated in order to assess the performance of the controllers in situations that facilitate the overheating of the heat transfer fluid.

All evaluated controllers were able to avoid overheating but presented varying performances for each simulation case. The hybrid controller presented itself as an interesting alternative as it obtained overall good performance while having relatively low computation times.

As proposal for future works, the inclusion of an explicit term of energy on the objective function in could be interesting to facilitate tuning. The usage of tuning techniques such as satisficing MPC can be interesting for obtaining a flexible tuning strategy for the controllers.

Acknowledgments

This work has been developed within the context of all activities related to the R&D project registered with ANEEL under the code PD-00553-0042/2016 and sponsored by Petroleo Brasileiro (PETROBRAS). J. E. Normey-Rico thanks CNPq for financial support, project 305785/2015-0.

References

Andrade, G. A., Pagano, D. J., Álvarez, J. D., Berenguel, M. 2013. A practical NMPC with robustness of stability applied to distributed solar power plants. Solar Energy 92, 106-122.

Camacho, Eduardo F., Bordons Alba, Carlos. 2007. Model Predictive Control. Ed. Springer-Verlag, London.

Carmona, R., 1985. Analysis, Modeling and Control of a Distributed Solar Collector Field with a One-axis Tracking System, Spanish: University of Seville, Spain.

Elias, T. de A., Mendes, P. da C., Normey-Rico, J. E. 2019. Hybrid predictive controller for overheating prevention of solar collectors. Renewable Energy 136, 535-547.

Frank, E., Mauthner, F., Fischer, S. 2015. Overheating prevention and stagnation handling in solar process heat applications. nt. Energy Agency Sol. Heat. Cool. Task 49.

Plucênio, A., Pagano, D., Bruciapaglia, A., and Normey-Rico, J. E. 2007. A practical approach to predictive control for nonlinear processes. IFAC Proceedings 40(12), 210–215.

Sánchez, A. J., Gallego, A. J., Escaño, J. M., Camacho, E. F. 2018. Event-based MPC for defocusing and power production of a parabolic trough plant under power limitation. Solar Energy 174, 570–581.